ER-60 Domains Responsible for Interaction with Calnexin and Calreticulin

Reiko Urade,* Hirokazu Okudo, Hiroyuki Kato, Tatsuya Moriyama, and Yukino Arakaki

Graduate School of Agriculture, Kyoto University, Uji, Kyoto 611-0011, Japan

Received April 5, 2004; Revised Manuscript Received May 14, 2004

ABSTRACT: ER-60 is a thiol oxidoreductase family protein of the endoplasmic reticulum that facilitates the oxidative folding of glycoproteins via interaction with calnexin (CNX) and calreticulin (CRT). In this study, we tried to identify the site of interaction with CNX and CRT in the ER-60 molecule. ER-60 was shown to be composed of at least four domains, named a, b, b′, and a′, by limited proteolysis. Recombinant fragments of ER-60, a, b′, and a′c, were each expressed in *Escherichia coli* as an individual soluble folded protein that underwent a cooperative unfolding transition along a urea gradient. These fragments each gave the circular dichroism (CD) spectrum of the folded protein. On the other hand, fragment b, which did not undergo the cooperative unfolding transition along a urea gradient gel, did not show any sign of the folded structure on the CD measurement. However, subtraction of the spectra showed that the b domain was folded in wild-type ER-60 or abb′. Both a and a′c, which have a catalytic center CGHC motif, showed activity almost equivalent to half of that of wild-type ER-60. Extension from a or a′c to ab and abb′ or b′a′c had little effect on their isomerase activity, suggesting that the b and b′ domains hardly contribute to the catalytic activity of ER-60. The contribution of both the b and b′ domains to the binding with CNX and CRT was revealed by surface plasmon resonance analysis and oxidative-refolding experiments of monoglucosylated RNase B with addition of the luminal domain of CNX.

Secretory and membrane proteins become folded with the assistance of molecular chaperones and other folding factors in the endoplasmic reticulum (ER).[1] In many cases, protein folding in the ER is accompanied by N-glycosylation and the formation of disulfide bonds. The formation of disulfide bonds between correct pairs of cysteine residues in a nascent polypeptide chain is thought to be catalyzed by protein disulfide isomerase (PDI) (*1*, *2*) and other member of its family, such as ER-60 (also known as ERp57, ERp60, ERp61, GRP58, p58, HIP-70, or Q2) (*3*−*9*), P5 (*10*), Erp72 (*11*), PDIp (*12*), PDIr (*13*), ERp44 (*14*), and ERp18 (*15*), etc. in the ER. Among them, ER-60 has been shown to be a multifunctional protein, which exhibits disulfide bond isomerase activity (*7*, *16*), endoproteinase activity (*3*, *17*, *18*), and transglutaminase-like activity in vitro (*19*). The isomerase activity of the disulfide bond of ER-60 (ERp57), which may be low compared to that of PDI, has been shown to increase remarkably with addition of the luminal domain of calnexin (CNX), a lectin-type molecular chaperone (*20*), or calreticulin (CRT), a soluble ER luminal paralog of CNX (*21*). In the ER, binding of ER-60 (ERp57) to newly synthesized glycoproteins has been demonstrated in combination with either CNX or CRT (*22*, *23*). Furthermore, the glycoprotein has been shown to form mixed disulfides with ER-60 (ERp57) depending on the monoglucosylated N-linked glycan, which is the ligand of either CNX or CRT (*24*, *25*). Overall, ER-60 is thought of as an expert in the introduction of disulfide bonds into glycoproteins through the interaction with either CNX or CRT. CNX is an integral type-I ER membrane protein comprising a C-terminal cytosolic domain (485−573), a transmembrane domain (463−484), and an N-terminal luminal domain (1−462), exhibiting sequence similarity with CRT (*26*). The three-dimensional structure of the luminal domain of CNX (61−458) has been solved by X-ray crystal structure analysis (*27*, *28*). It shows that an extended hairpin fold arm, which is called the proline-rich P domain, is inserted into a compact globular lectin domain. The ternary structure of the CRT P domain (189−288), which has been solved by nuclear magnetic resonance (NMR) spectroscopy in solution, shows an unusual extended hairpin fold similar to the P domain of CNX (*29*, *30*). TROSY−NMR analysis and protein engineering studies have demonstrated that ER-60 interacts with the tip of the hairpin structure of the P domain of CRT (*31*, *32*). On the other hand, the ternary structure of ER-60 is unclear and the site of ER-60 responsible for interaction with CNX and CRT has not been clarified. ER-60 is assumed to comprise four structural domains, a, b, b′, and a′, and a C-terminal extension, as judged on alignment with the primary structure of PDI (*33*−*35*). In particular, the homologous a and a′ domains of ER-60, which each contain a thioredoxin-like active-site motif, show significant sequence identity to the a and a′ domains of PDI. The recombinant fragment a of human PDI has been shown to have a characteristic thioredoxin fold ($\beta\alpha\beta\alpha\beta\beta\alpha$) by NMR analysis (*36*). Recombinant fragment S^{373}−E^{492} of ER-60 (ERp57), corresponding to the putative a′ domain region, has also been shown to be

* To whom correspondence should be addressed. Phone: 81-774-38-3757. Fax: 81-774-38-3758. E-mail: urade@soya.food.kyoto-u.ac.jp.

[1] Abbreviations: AMS, 4′-maleimidylstilbene-2,2′-disulphonic acid; CD, circular dichroism; CNX, calnexin; CRT, calreticulin; ΔTMC, recombinant luminal domain of calnexin; DTT, dithiothreitol; ER, endoplasmic reticulum; GSH, glutathione; GSSG, glutathione disulfide; HEPES, [4-(2-hydroxyethyl)-1-piperazinyl]ethanesulfonic acid; IPTG, isopropyl thiogalactoside; NMR, nuclear magnetic resonance; PAGE, polyacrylamide gel electrophoresis; PCR, polymerase chain reaction; PDI, protein disulfide isomerase; PVDF, poly(vinylidene difluoride); RNase, ribonuclease; SPR, surface plasmon resonance; Tris, tris-(hydroxymethyl) aminomethane.

10.1021/bi0493315 CCC: $27.50 © 2004 American Chemical Society
Published on Web 06/18/2004

folded into a thioredoxin-like form ($\beta\alpha\beta\alpha\beta\beta\beta\alpha$) similar to that of PDI (*37*), suggesting functional similarity between the a and a′ domains of both PDI and ER-60. The high-resolution NMR structure of fragment b of PDI has shown that the b domain folds into a structure similar to that of the a domain, despite the low degree of sequence similarity between these domains (*38*, *39*). Judging from the similarity between the a and a′ domains or the b and b′ domains of PDI, all of these domains are thought to fold into a thioredoxin-like form. The results obtained in protein engineering studies indicate that the b′ domain of PDI carries the principle peptide-binding site of PDI (*40*, *41*). The sequences of the putative b and b′ domains and C-terminal extension of ER-60 are hardly homologous to those of PDI. Such differences between the primary structures of ER-60 and PDI are assumed to cause the differences in their functions. However, the details of the relationships between the sequences and functions of ER-60 and PDI are unclear.

Among the characteristic functions of ER-60, its cooperation with CNX and CRT prompted us to investigate which domain of ER-60 is responsible for the interaction with these molecular chaperones. In this study, we revealed the domain boundaries of ER-60. With this structural information, we employed recombinant fragments of ER-60 to localize the site of its CNX or CRT binding.

EXPERIMENTAL PROCEDURES

Materials. [α-^{32}P]ATP (110 TBq/mmol) was obtained from NEN Life Science Products Inc. UDP-[^{3}H] glucose (925 GBq/mmol) and MonoQ, ConA Sepharose and DEAE columns were purchased from Amersham Biosciences. AF-heparin Toyopearl 650M resin and a TSK gel G3000SW HPLC column were obtained from TOSOH (Tokyo, Japan). *Escherichia coli* expression vector pET-30Xa/LIC and His-Bind quick cartridges were purchased from Novagen. The pTYB-1 vector and chitin beads were from New England BioLabs. Bovine PDI was obtained from TAKARA Shuzou (Kyoto, Japan) and repurified by hydroxyapatite column chromatography as described previously (*18*). CRT was purified from rat liver as described previously (*3*). Poly(vinylidene difluoride) (PVDF) protein sequencing membranes were obtained from Bio-Rad. CNX-N antiserum was purchased from StressGen Biotechnologies Corp. Horseradish peroxidase-conjugated rabbit Ig antiserum was obtained from Promega. Trypsin, chymotrypsin, and V8 protease were purchased from Boehringer Mannheim. Ribonuclease (RNase) A, RNAse B, and Ponceau S were from Sigma. 4′-Maleimidylstilbene-2,2′-disulfonic acid (AMS) was purchased from Molecular Probes (Leiden, The Netherlands). All other chemicals were of reagent grade.

Peptide Mapping of ER-60. Expression and purification of recombinant wild-type ER-60 were carried out as described previously (*18*). The purified ER-60 (150 μg) was digested with trypsin (3 μg) in a 50 mM tris(hydroxymethyl) aminomethane (Tris)/HCl buffer at pH 8 and 25 °C for 60 min, with V8 protease (1.5 μg) in a 125 mM Tris/HCl buffer at pH 8.5 and 25 °C for 60 min, or with chymotrypsin (1.5 μg) in a 100 mM Tris/HCl buffer at pH 8.5, containing 10 mM $CaCl_2$ at 25 °C for 30 min. The peptides produced were separated by SDS−polyacrylamide gel electrophoresis (PAGE) (15% gel), transferred to PVDF membranes, and then stained with Ponceau S. N-terminal amino acid sequencing of each peptide was carried out with a Protein Sequencer Model 492 (Applied Biosystems), as described previously (*3*).

Construction of Expression Vectors for Recombinant Fragments of ER-60. The amino acid sequence of each polypeptide construct used in this study is shown in Figure 2A. Appropriate DNA fragments were amplified by the polymerase chain reaction (PCR) from a cDNA clone of human ER-60 (*18*). The primers of the DNA sequence for the N or C terminus of the recombinant a, b, b_L, b′, ab_L, or abb′ fragment contained a *Nde*I or *Sap*I restriction site, respectively. The PCR fragments produced were digested with *Nde*I and *Sap*I and then cloned into the corresponding site of pTYB-1, which allowed the fusion of a self-cleavable intein tag containing the chitin-binding domain to the C terminus of a target protein (*42*). For the construction of expression vectors for the recombinant a′c and b′a′c fragments, which had a *Nde*I restriction site in their sequences, a sequence TG, which becomes a part of an initiator ATG methionine codon after cloning into pTYB-1, was added to the 5′ termini of the PCR primers. The PCR fragments produced were digested with *Sap*I and then cloned into pTYB-1, which was digested with *Nde*I, blunt-ended with T4 DNA polymerase, and then digested with *Sap*I. The inserts in the expression vectors were sequenced by the fluorescence dideoxy chain termination method (Perkin−Elmer, Applied Biosystems).

Expression and Purification of Recombinant Fragments of ER-60. The expression of ER-60 fragments was carried out in *E. coli* strain BL21(DE3). Gene expression was induced by the addition of 0.4 mM isopropyl thiogalactoside (IPTG) for 4 h. Cells from 2 L of culture were resuspended in 50 mL of a 20 mM [4-(2-hydroxyethyl)-1-piperazinyl]-ethanesulfonic acid (HEPES) buffer at pH 8.0, containing 0.5 M NaCl and 1 mM EDTA (buffer A) at 4 °C, and then disrupted by sonication. The lysed cells were centrifuged at 10000*g* for 30 min at 4 °C. The clarified extract was loaded onto a chitin column. The column was washed with 10 bed volumes of buffer A to remove unbound *E. coli* proteins and then equilibrated against 50 mM dithiothreitol (DTT) in buffer A. On-column cleavage of each recombinant fragment of ER-60 from the intein tag was carried out at 4 °C for ∼16−40 h. The cleaved recombinant fragments were eluted from the column with buffer A, concentrated with a Centriprep-10 (Millipore), and then dialyzed against a 20 mM Tris/HCl buffer at pH 7.4, containing 0.15 M NaCl and 10% glycerol (buffer B), at 4 °C overnight. The dialyzed sample was subjected to gel-filtration chromatography on a TSK gel G3000SW column equilibrated with buffer B. Corresponding fractions were combined, concentrated, and stored at −80 °C.

Construction of an Expression Vector for the Recombinant Luminal Domain of Human CNX. The plasmids containing cDNA of human CNX (*kaia* 4724) were obtained from the Japanese Collection of Research Bioresources Gene Bank (Tokyo, Japan) (*43*). An expression vector for the recombinant luminal domain of CNX (ΔTMC), which corresponds to residues 1−462 of mature CNX (*44*), was constructed as described below. For cloning into an expression vector, DNA fragments were amplified by PCR with the primers of the DNA sequence encoding the N or C terminus of ΔTMC, containing a *Nde*I or *Xho*I restriction site. The PCR fragments produced were digested with *Nde*I and *Xho*I and then cloned

into pET-30Xa/LIC, digested with *Nde*I and *Xho*I. This expression vector, pET-30/ΔTMC, allows for the fusion of the histidine tag LEHHHHHH to the C terminus of ΔTMC.

Expression and Purification of ΔTMC. BL21(DE3) cells were transformed with pET-30/ΔTMC. The expression of ΔTMC was induced by the addition of 0.4 mM IPTG for 4 h. ΔTMC was produced as a soluble protein in *E. coli*. The cells from 1 L of culture broth were collected by centrifugation, disrupted by sonication in 40 mL of a 20 mM Tris/HCl buffer at pH 7.9, containing 5 mM imidazole, 0.5 M NaCl, and 1 mM $CaCl_2$ (binding buffer), and then centrifuged at 10000*g* for 30 min at 4 °C. The supernatant was applied to a His-Bind quick cartridge. After the cartridge was washed with the binding buffer, ΔTMC was eluted with the binding buffer containing 1 M imidazole, concentrated with a Centriprep-10, and then subjected to gel-filtration chromatography on a TSK gel G3000SW column equilibrated with buffer B, containing 1 mM $CaCl_2$. ΔTMC was eluted in both the void volume and the inside volume fractions corresponding to 180 kDa. The 180-kDa fractions were collected and used for the following assays. ΔTMC was confirmed to have an initial methionine residue by N-terminal sequencing.

ATP-Binding Assay of ΔTMC. The ATP-binding assay was performed as described by Ou et al. (*45*). Briefly, the purified ΔTMA (5 μg/10 μL) was incubated in 2.5 μCi/10 μL (25 μM) [α-^{32}P]ATP in a 20 mM HEPES buffer at pH 7.5, containing 50 mM NaCl, 2 mM $CaCl_2$, and 10 mM $MgCl_2$, in the presence or absence of 10 mM DTT at 20 °C for 15 min and then exposed to UV radiation at 30 mJ for 1−5 min. Samples were subjected to SDS−PAGE (10% acrylamide gel) and then staining with Coomassie Brilliant Blue R-250 followed by autoradiography.

Urea-Gradient Gel Electrophoresis. Urea-gradient gel electrophoresis was carried out as described by Creighton (*46*). Briefly, a transverse urea gradient in a polyacrylamide slab gel containing a 0.375 M Tris/HCl buffer at pH 8.8, with a running buffer comprising a 25 mM Tris-glycine buffer at pH 8.3, was formed with a first solution comprising 15% acrylamide and no urea and a second solution comprising 11% acrylamide and 8 M urea. A total of 100 μg of protein was electrophoresed on the gel at 10 °C for 4−6 h, followed by staining with a silver-staining kit (Bio Rad).

Far-UV Circular Dichroism (CD) Spectra Analysis. CD spectra were measured with a Spectropolarimeter J-720 (JASCO Corporation, Tokyo, Japan) in a 1-mm path-length cell at 23 °C. The proteins were dissolved in a 20 mM potassium phosphate buffer at pH 7.4. Wild-type ER-60 was converted to the thiol (reduced) or disulfide (oxidized) form of the catalytic CGHC motif by dialysis against a 20 mM potassium phosphate buffer at pH 7.4, containing 5 mM DTT or 0.1 mM glutathione disulfide (GSSG) overnight. The reduced or oxidized ER-60 was then dialyzed against a 20 mM potassium phosphate buffer at pH 7.4. For the determination of the oxidation state of ER-60, ER-60 or the mutant ER-60 (C60A/C409A) (*47*) was incubated in an 80 mM Tris/HCl buffer at pH 6.8, containing 2% SDS with or without 25 mM AMS at room temperature for 30 min and at 37 °C for 10 min. Samples were resolved by SDS−PAGE (7% acrylamide gel) and then stained with Coomassie Brilliant Blue R-250.

Oxidative Refolding of RNase A. Reduced RNase A was prepared as described by Creighton (*48*). Each reaction mixture comprised 200 mM HEPES at pH 7.5, 150 mM NaCl, 2 mM $CaCl_2$, 0.5 mM GSSG, 2 mM glutathione (GSH), 72 μM reduced RNase A, and 3.5 μM recombinant fragment of ER-60. The reaction mixture was incubated at 25 °C for 0 or 40 min. An aliquot (16 μL) of the reaction mixture was removed, and RNase A activity was measured spectrophotometrically at 284 nm with cytidine2′:3′-cyclic monophosphate as the substrate (*49*).

Preparation of Monoglucosylated RNase B. RNase B was monoglucosylated as described by Zapun et al. (*50*). RNase B was reduced and denatured by incubation in a 0.1 M Tris/HCl buffer at pH 8, containing 6 M guanidine chloride and 20 mM DTT for 2 h at 25 °C. The unfolded RNase B was desalted in 0.1% trifluoroacetic acid on a NAP-5 column and then freeze-dried. The unfolded RNase B (900 μg) was dissolved in 300 μL of a 30 mM Tris/HCl buffer at pH 8, containing 10 mM $CaCl_2$, 300 μM 1-deoxynojirimycin, 14 μM UDP-[^{3}H] glucose (5.3 MBq), and 190 μg of UDP−glucose:glycoprotein glucosyltransferase, which was purified from rat liver by sequential chromatographies on DEAE, Con A Sepharose, and Mono Q columns (*51*), and then incubated at 37 °C for 2.5 h. After the reaction, RNase B was incubated in a 0.1 M Tris/HCl buffer at pH 8, containing 6 M guanidine chloride, 20 mM DTT, and 300 mM 1-deoxynojirimycin at 25 °C for 20 min, desalted in 0.1% trifluoroacetic acid on a NAP-5 column, and then freeze-dried.

Oxidative Refolding of Monoglucosylated RNase B. Oxidative refolding of unfolded [^{3}H]-monoglucosylated RNase B was carried out as described by Zapun et al. (*50*). Refolding was initiated by dissolving the freeze-dried RNase B (60 μM) in a 20 mM Tris/HCl buffer at pH 7.5, containing 150 mM NaCl, 2 mM $CaCl_2$, 0.5 mM GSSG, 2 mM GSH, 300 μM 1-deoxynojirimycin, and 0.76 μM ER-60 or domain protein with or without 12 μM ΔTMC. The reaction mixture was incubated at 25 °C for 0, 20, 40, or 80 min. An aliquot was removed, reacted with 0.25 volumes of 0.5 M iodoacetamide in a 1.5 M Tris/HCl buffer at pH 8.7 and 25 °C for 5 min and then subjected to low pH nondenaturing PAGE (*20*, *52*). [^{3}H]-monoglucosylated RNase B in the gel was detected by fluorography with ENLIGHTING (NEN Life Science Products, Inc.).

Analyses of Protein−Protein Interactions with BIAcore. The BIAcore 2000 machine, CM5 sensor chips, and analysis program were all from Pharmacia Biosensor. The sensor chip was activated with a 1:1 mixture of *N*-hydroxysuccinimide/*N*-ethyl-*N*′-(3-dimethylaminopropyl)-carbodiimide hydrochloride, following the instructions of the manufacturer. The purified protein was immobilized in a 10 mM sodium acetate buffer at pH 4.0, and the remaining binding sites were blocked with 1 M ethanolamine at pH 8.5. The control channel on the sensor chip was activated and blocked using amine-coupling reagents, without immobilization of the protein. The binding of proteins to this control channel was subtracted from the specific binding. The experiments were performed at 20 °C with a 10 mM HEPES buffer at pH 7.0, containing 150 mM NaCl, 2 mM $CaCl_2$, and 0.05% Tween 20 (running buffer) at the flow rate of 10 μL/min. The running buffer was also used for diluting the samples for injection.

Other Procedures. The concentrations of proteins were measured by amino acid analysis of the protein samples supplemented with γ-aminobutyric acid as an internal

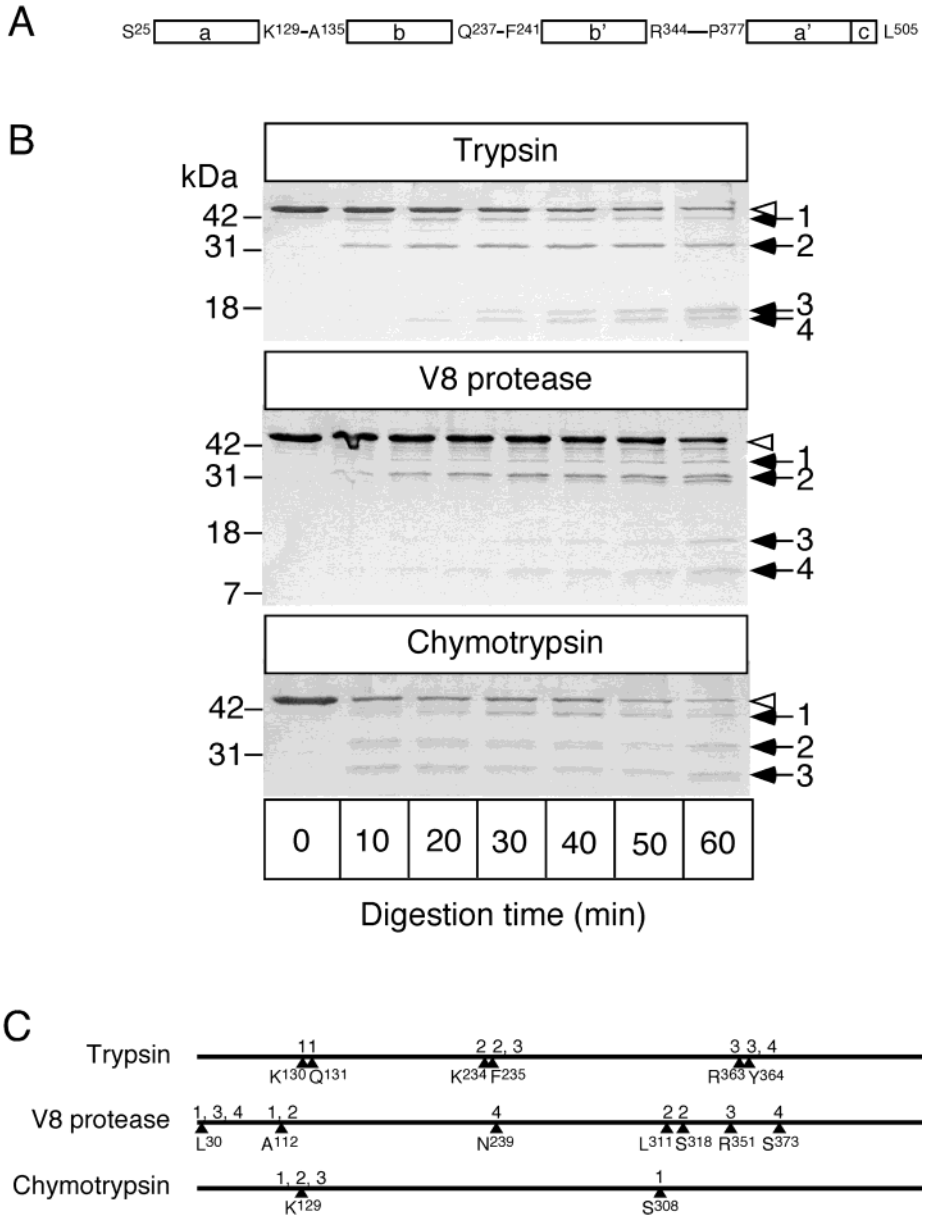

FIGURE 1: Identification of proteolytic cleavage sites in ER-60. (A) Domain structure of ER-60 predicted by alignment with the primary structure of PDI (*33*). (B) Recombinant human ER-60 (50 μg) was digested with trypsin (1 μg), V8 protease (0.5 μg), or chymotrypsin (0.5 μg) in 100 μL of a 0.1 M Tris/HCl buffer at pH 8 and 25 °C. A total of 10 μL was removed from the reaction mixture after incubation for 0, 10, 20, 30, 40, 50, or 60 min and then subjected to SDS−PAGE (15% gel). The proteins were stained with CBB-R250. The N-terminal amino acid sequences of numbered materials (closed arrowheads) were determined as described under the Experimental Procedures. Open arrowheads indicate the band of intact ER-60. (C) Cleavage sites (closed arrowheads) by digestion of ER-60 with trypsin, V8 protease, or chymotrypsin. The N-terminal amino acids of the peptide fragments, which were produced on protease digestion, are each indicated as a cleavage site. The number above each cleavage site is the number of the band in the panel (B).

standard. Western blotting was carried out with CNX-N antiserum. Briefly, proteins separated by SDS−PAGE were blotted onto PVDF membranes and then immunostained with horseradish peroxidase-conjugated rabbit Ig antiserum as second antibodies, using Renaissance Chemiluminescence Reagent (DuPont NEN).

RESULTS

Domain Structure of ER-60. The domain structure of ER-60 was predicted to be similar to that of PDI with a linear sequence of four domains in an a−b−b′−a′ pattern from the sequence homology between the two proteins (Figure 1A). However, there was no direct information on the domain structure of ER-60. Hence, we started a study in which recombinant ER-60 was subjected to limited proteolysis with trypsin, V8 protease, or chymotrypsin for various incubation times to define the domain boundaries of ER-60. ER-60 was gradually degraded depending the incubation time with each protease, with smaller sized peptide fragments being generated (Figure 1B). The sites of cleavage by the proteases were determined by N-terminal sequencing of the peptide fragments blotted onto a PVDF membrane after SDS−PAGE. The cleavage sites resided in three narrow regions, A^{112}−Q^{131}, K^{234}−N^{239}, and S^{308}−S^{373} (Figure 1C). These regions overlap the putative boundary regions between the a and b, b and b′, and b′ and a′ domains, respectively. These results suggest that ER-60 has a linear sequence of four domains in an a−b−b′−a′ pattern.

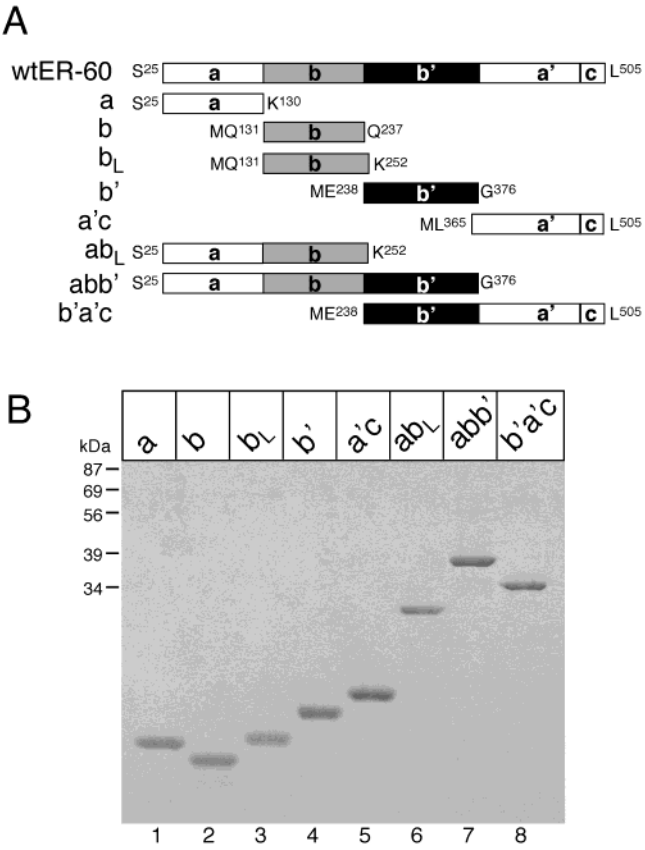

FIGURE 2: Expression of recombinant fragments of ER-60. (A) Recombinant fragments of ER-60 used in this study. The nomenclature adopted is based upon the hypothesized domain structure of ER-60. The N- or C-terminal amino acid residue of each domain is given on the left or right side of the domain bar, respectively. M donates an initial methionine residue. (B) Purified recombinant fragments of ER-60. Recombinant fragments of ER-60 were expressed with IPTG for 4 h. Each fragment was self-cleaved from an intein tag by treatment with DTT on a chitine column and then subjected to TSK gel G3000 column chromatography as described under the Experimental Procedures. The purified fragment (3 μg of protein) was separated by SDS−PAGE, followed by staining with CBB-R250.

Expression of Recombinant Fragments of ER-60. The polypeptide fragments of ER-60 used in this study are listed in Figure 2A. Basically, the polypeptide fragments produced were chosen to contain all of the residues of each putative domain plus the flanking residues. Each polypeptide fragment was expressed as a fusion protein with an intein tag and then purified as an intein-tagless polypeptide by the self-cleavage method, as described under the Experimental Procedures (Figure 2B). All recombinant fragments were expressed as a soluble form in *E. coli* and eluted as a single nonaggregated form on gel-filtration column chromatography. The N-terminal amino acids of a, ab_L, and abb′ were serine, which is the N-terminal residue of mature ER-60, after the processing of the signal sequence in the ER. The initial methionine residue of other recombinant proteins was not removed from their N termini in *E. coli*.

To determine whether each recombinant fragment of ER-60 is an autonomously folded unit of ER-60, urea-gradient gel analysis and CD spectral analysis were carried out. Three fragments, a, b′, and a′c, exhibited the cooperative folding transition on urea-gradient gel electrophoresis (parts A, D, and E of Figure 3), and gave a CD spectrum typical of a

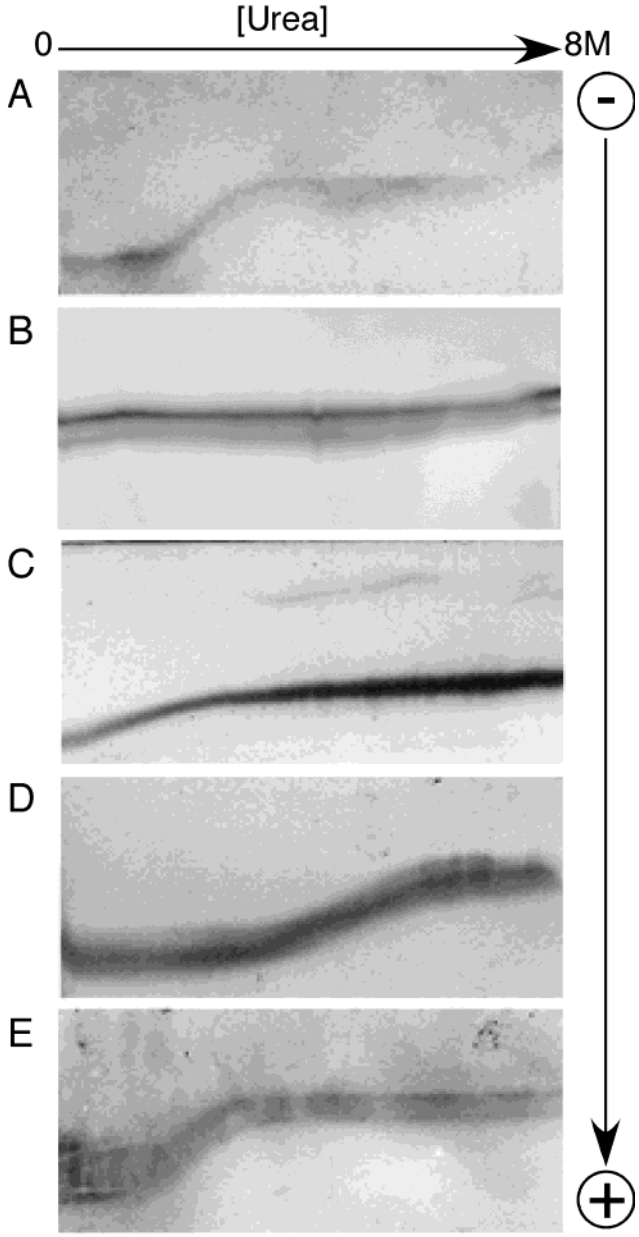

FIGURE 3: Urea-gradient analysis of recombinant fragments of ER-60. Each fragment, a (A), b (B), b_L (C), b′ (D), or a′c (E) (100 μg of protein), was electrophoresed on urea-gradient gel as described under the Experimental Procedures. Proteins were stained with silver.

folded protein (Figure 4A). On the other hand, fragment b did not undergo the cooperative folding transition on urea-gradient gel electrophoresis (Figure 3B). In addition, fragment b gave a CD spectrum without substantial structural indications (Figure 4A). From these results, the unfolding of fragment b was assumed to be caused by misidentification of the boundary between the b and b′ domains. Then, a new recombinant fragment, b_L, which is fragment b elongated at the C terminus from Gln^{237} to Lys^{252}, was designed and analyzed. The Lys^{252} position was chosen as the last amino acid residue in the turn region behind Gln^{237} based on the prediction of the secondary structure by the Chou and Fasman method (*53*). Again, neither the cooperative folding transition on urea-gradient gel electrophoresis (Figure 3C) nor a CD spectrum with structural indications (Figure 4A) was obtained on analysis of b_L. Extension from b_L to ab_L

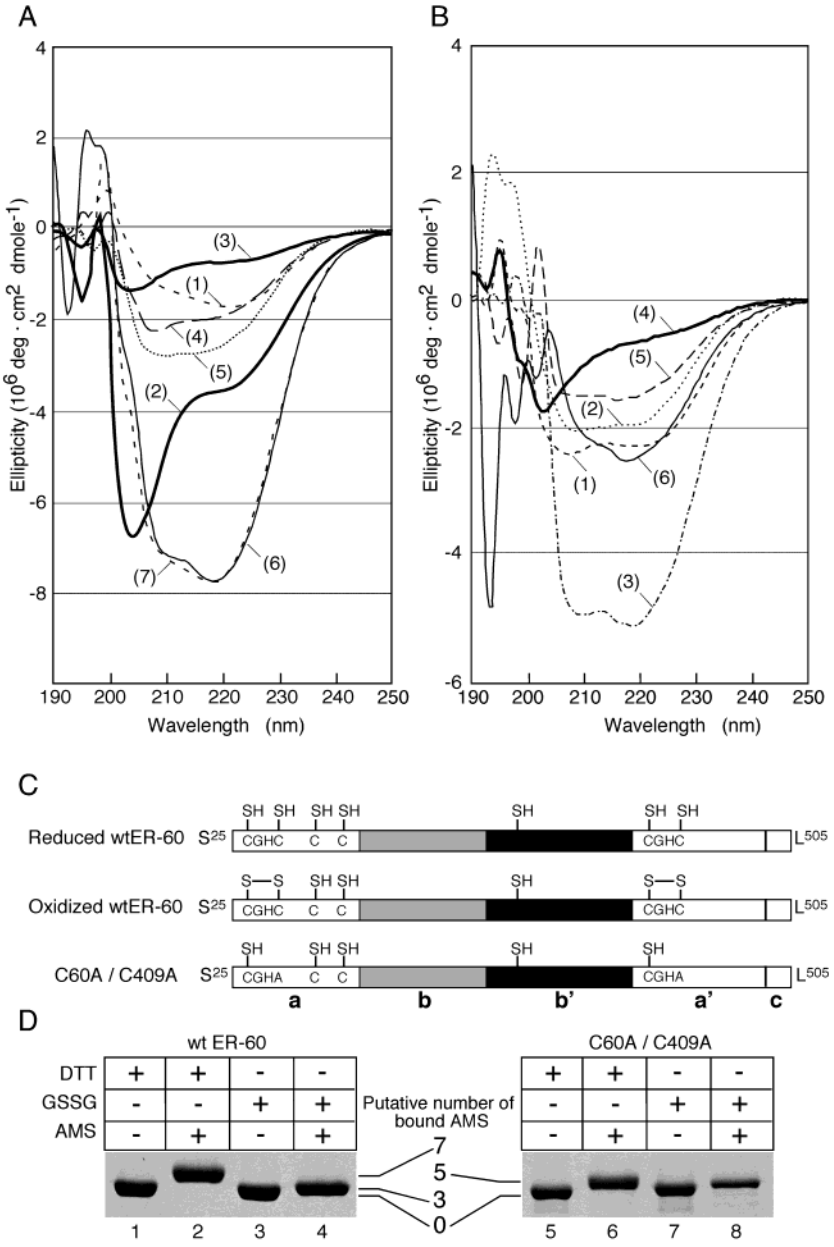

FIGURE 4: CD spectra of recombinant fragments of ER-60. (A) CD spectra of a (1), b (2), b_L (3), b′ (4), a′c (5), and the dithiol (6) and disulfide (7) forms of wild-type ER-60 were obtained as described under the Experimental Procedures. (B) CD spectra of ab_L (1), b′a′c (2), and abb′ (3) were obtained, and then subtraction spectra, ab_L − a (4), abb′ − a − b′ (5), and wild-type ER-60 − a − b′a′c (6), were calculated. (C) Expected redox states of ER-60 and C60A/C409A reduced or oxidized with DTT or GSSG. (D) ER-60 (lanes 1−4) and C60A/C409A (lanes 5−8) were treated with DTT (lanes 1, 2, 5, and 6) and GSSG (lanes 3, 4, 7, and 8). Free protein thiols were modified with AMS (lanes 2, 4, 6, and 8) or not modified with AMS (lanes 1, 3, 5, and 7) as described under the Experimental Procedures. Samples were resolved by SDS−PAGE.

had no effect on the unfolding of the b region. Subtraction of the spectrum of fragment a from that of ab_L, corresponding to the spectrum of the b region, showed no structural indications (Figure 4B). However, subtraction of the spectra of fragments a and b′a′c from that of wild-type ER-60 yielded a spectrum with structural indications (Figure 4B). In addition, subtraction of the spectra of fragments a and b′ from that of abb′ also yielded a spectrum characteristic of a folded protein (Figure 4B), suggesting that the b region has a folded structure in ER-60.

ER-60 contains two CGHC motifs, which are catalytic centers in the a and a′ domains. In the ER, an oxidized disulfide form of ER-60 is thought to be the form exhibiting oxidative-folding activity. To determine whether there is any difference between the structures of the reduced dithiol and oxidized disulfide forms of ER-60, the purified ER-60 was treated with DTT or GSSG. To confirm the redox states of the two CGHC motifs in ER-60, each sample was treated with the alkylating agent AMS and then the electrophoretic mobility of ER-60 was determined under nonreducing conditions (Figure 4D). ER-60 treated with DTT migrated more slowly after AMS modification. ER-60 treated with GSSG also showed a smaller but detectable mobility shift after AMS modification. These results suggested that a intramolecular disulfide bond(s) was formed in the ER-60 molecule with GSSG treatment. To confirm that the disulfide bonds were formed by oxidations of the two cysteine residues in each CGHC motif, the mobility shift of an ER-60 cysteine-

Table 1: Oxidative Refolding of Reduced RNase A Caused by Recombinant Fragments of ER-60

protein	% activity	protein	% activity
ER-60 variant		PDI variant	
wild type	100[a]	wild type (bovine)	431[a]
a	48[a]	wild type (rat)	290[b]
ab_L	67[a]	a	12[b]
abb′	56[a]	ab	19[b]
a′c	40[a]	abb′(Xa′X)	116[c]
b′a′c	56[a]	a′	9[b]
		b′a′c	110[b]

[a] Oxidative refolding of RNase A was assayed as described under the Experimental Procedures. 100% corresponds to the activity of ER-60 (0.1485 mol of RNase A min^{-1} mol of $protein^{-1}$). Values represent the means of three experiments. [b] Data from Xiao et al. (*54*). [c] Data from Walker et al. (*55*). Xa′X represents an active site in which the catalytic CGHC motif of the a′ domain has been inactivated by mutation to SGHS.

alanine replacement mutant with the CGHC motif, C60A/C409A, was analyzed. The mobility shifts of C60A/C409A treated with DTT and GSSG after AMS modification are the same, suggesting that disulfide bonds were formed between the two cysteine residues in each CGHC motif of ER-60 on treatment with GSSG. The AMS-modified C60A/C409A migrated more rapidly than the reduced and AMS-modified ER-60 but migrated more slowly than the oxidized and AMS-modified ER-60. These findings suggested that both CGHC motifs of ER-60 were oxidized with GSSG treatment and that the small mobility shift of the oxidized ER-60 after AMS modification was due to the modification of cysteine residues other than those in the CGHC motif (Figure 4C). The CD spectrum of the reduced or oxidized ER-60 was monitored. No difference was observed (Figure 4A).

Oxidative Refolding of Reduced RNase A Caused by Recombinant Fragments of ER-60. The activity of recombinant fragments of ER-60, i.e., the catalysis of oxidative refolding of the reduced, denatured RNase A, was measured. The formation of native disulfide bonds in the RNase A was followed as the rate of hydrolysis of 2′,3′-cCMP. Activity was detected for all of the constructs containing the a or a′ domain. The activity of wild-type ER-60 was only 23 or 34% of that of bovine or rat PDI (Table 1). Fragments a and a′c showed activity almost equivalent to half (48 and 40%) of that of wild-type ER-60, suggesting that the a and a′ domains can independently catalyze the isomerization of disulfide bonds. The b′ domain of PDI has been reported to function as the principal substrate-binding domain (*40*, *41*). Hence, the activity of fragment abb′ or b′a′c of PDI was about 10-fold that of fragment a or a′ of PDI. On the other hand, the contribution of the b′ domain to the isomerase activity of ER-60 was very small; thus, its isomerase activity was hardly affected by extension from a or a′c to abb′ or b′a′c. The b′ domain of ER-60 will not function as a substrate-binding site, at least not for refolding of unfolded RNase A.

Interaction of Recombinant Fragments of ER-60 with CNX and CRT. There are two kinds of ER-60-binding sites on CNX and CRT, i.e., Zn^{2+}-dependent and -independent ones (*30*, *32*, *56*). The Zn^{2+}-dependent-binding site was found in vitro in the presence of a high concentration of Zn^{2+} (>100 μM), which causes changes in the conformation of both CRT and ER-60 (*56*, *57*). The physiological significance of this interaction is unclear, although Zn^{2+} has been reported to

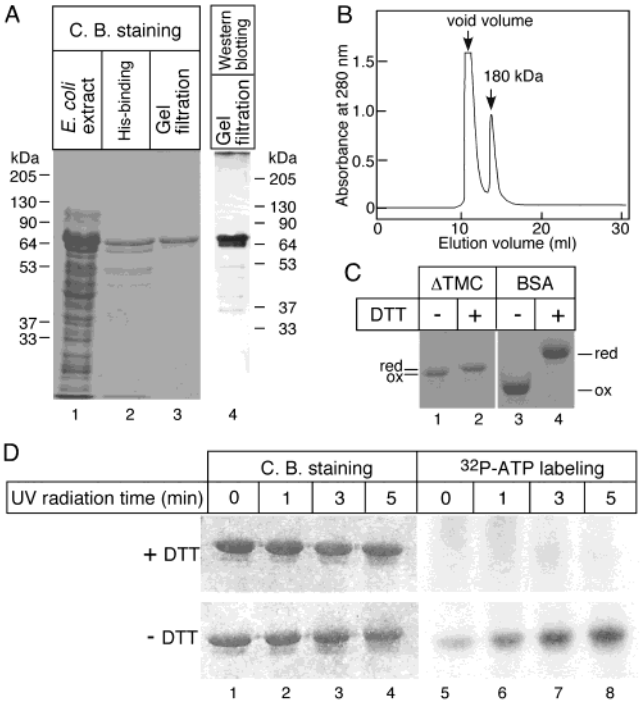

FIGURE 5: Expression and purification of ΔTMC. (A) SDS−PAGE (10% gel) analysis of pooled fractions at various stages of purification of ΔTMC. Extract of *E. coli* in which ΔTMC was expressed (lane 1); pooled fractions obtained on His-tag-binding column chromatography (lane 2); and fractions obtained on TSK gel G3000SW gel-filtration column chromatography (lanes 3 and 4). Proteins were stained with CBB-R250 (lanes 1−3) or immunostained with anti-CNX (lane 4) as described under the Experimental Procedures. (B) Gel-filtration column chromatogram of ΔTMC expressed in *E. coli*. The pooled fractions obtained on His-tag chromatography were subjected to TSK gel G3000SW gel-filtration column chromatography as described under the Experimental Procedures. The elution of proteins was followed as the UV absorption at 280 nm. (C) Disulfide bonding of ΔTMC. The purified 180 kD form of ΔTMC (2 μg of protein) or BSA (2 μg of protein), as a positive control, was separated by SDS−PAGE (7% gel) under nonreducing (lanes 1 and 3) or reducing (lanes 2 and 4) conditions, followed by staining with CBB-R250. A small difference in mobility was observed between the disulfide-bonded (ox) and reduced (red) forms of ΔTMC. (D) Binding of ATP to ΔTMC. The purified 180 kD form of ΔTMC was incubated with [α-^{32}P]ATP in the presence (upper panel) or absence (lower panel) of DTT and then exposed to UV radiation for 1 min (lanes 2 and 6), 3 min (lanes 3 and 7), or 5 min (lanes 4 and 8) or not exposed (lanes 1 and 5), as described under the Experimental Procedures. The proteins were separated by SDS−PAGE and then stained with CBB-R250 (lanes 1−4), followed by autoradiography (lanes 5−8).

be present within the ER (*58*). The Zn^{2+}-independent-binding site was shown to reside within the arm domains of CNX and CRT (*32*). These sites are thought to be used for the interaction of ER-60 in the ER. Therefore, in this study, the Zn^{2+}-independent interactions of ER-60 with CNX and CRT were analyzed. For binding experiments, the recombinant luminal domain of CNX, ΔTMC, was expressed in *E. coli* and then purified (Figure 5A). A total of 15% of the expressed ΔTMC, which comprises a lectin domain and an arm, was eluted in the inside volume fractions on the gel filtration corresponding to the size of 180 kD (Figure 5B). The rest of the ΔTMC soluble but aggregated form was eluted in the void volume from the gel-filtration column. The nonaggregated 180 kD form of ΔTMC was confirmed to have an inner molecular disulfide bond, which is essential for the native conformation of CNX and its ATP-binding

ability (*44*) (parts C and D of Figure 5). Thus, we examined the interactions of the nonaggregated 180 kD form of ΔTMC with recombinant fragments of ER-60 by surface plasmon resonance (SPR) analysis. Initially, the binding of ΔTMC to ER-60 immobilized on the surface of a chip was determined. When ΔTMC was passed over the chip, a time-dependent increase in the response was observed, indicating that ΔTMC became associated with ER-60 (Figure 6A). Association and dissociation of ΔTMC and ER-60 were not affected by the addition of ATP, which has been reported to enhance the binding of CNX with an unfolded polypeptide (*59*). Next, to identify the domain of ER-60 responsible for the interaction with CNX, we carried out SPR analysis of fragments of ER-60 with a ΔTMC chip (Figure 6B). When wild-type ER-60 was passed over the chip, association was observed. There was no difference between the association of the dithiol and disulfide forms of ER-60 with ΔTMC. No association of fragment a or a′c with ΔTMC was observed. A slight association of b′ or b′a′c with ΔTMC was detected, and a substantial association of fragment abb′ with ΔTMC was observed. Similar results were obtained on analysis of the interaction of ER-60 fragments with a CRT chip (Figure 6C).

The oxidative refolding of monoglucosylated RNase B caused by ER-60 in vitro has been shown to be accelerated through cooperation with ΔTMC (*20*). The effect of ΔTMC on the oxidative refolding of monoglucosylated RNase B caused by fragments of ER-60 containing the a or a′ domain was determined (Figure 7). The oxidative refolding of monoglucosylated RNase B was not observed in the absence of ER-60 or an ER-60 fragment regardless of the addition of ΔTMC. Slight refolding of the monoglucosylated RNase B was observed in the presence of wild-type ER-60 alone in the absence of ΔTMC. This activity was enhanced by the addition of ΔTMC. The activities of fragments a and b′a′c, which hardly associated with ΔTMC, shown with SPR analysis, were not enhanced by the addition of ΔTMC. On the other hand, the oxidative-refolding activity of abb′, which did associate with the ΔTMC, shown with SPR analysis, was enhanced by the addition of ΔTMC (Figure 7). These results suggest that both the b and b′ domains of ER-60 are essential for the association with CNX or CRT.

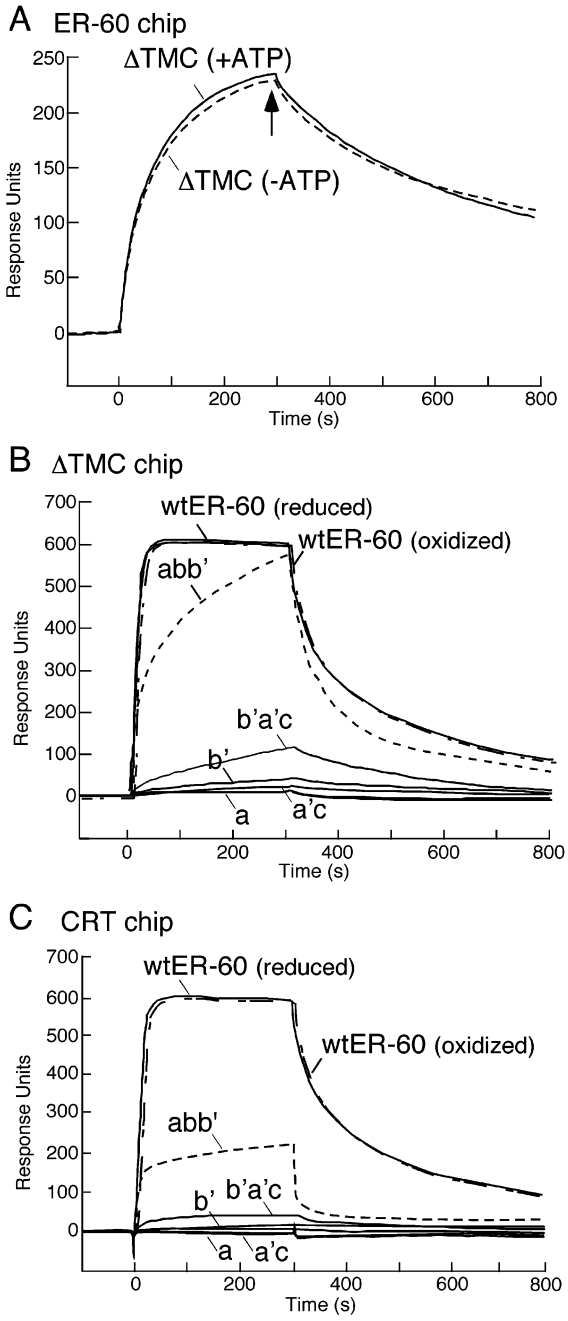

FIGURE 6: Examination of binding of CNX or CRT and recombinant fragments of ER-60 by SPR analysis. (A) ER-60 (26 fmol/mm^2) was immobilized on the surface of a SPR chip as described under the Experimental Procedures. At zero time, ΔTMC (1.8 μM) was added to the buffer solution that passed continuously over the chip. The experiments were performed in the presence or absence of 1 mM ATP and 2 mM $MgCl_2$ as described under the Experimental Procedures. At the time the curve began to fall (arrow), the ΔTMC solution was replaced by the buffer. The nonspecific response in a manner with a blank chip exposed has been subtracted from the response units shown. (B) ΔTMC (23 fmol/mm^2) was immobilized on the surface of a SPR chip, and then the on and off rates for the binding of recombinant fragments of ER-60 were recorded with the passage of 0.1 μM protein. (C) Rat CRT (20 fmol/mm^2) was immobilized on the surface of a SPR chip, and the on rates and off rates for the binding of recombinant fragments of ER-60 were recorded by the flow of 0.42 μM protein.

DISCUSSION

In the ER, inner- and interdisulfide bonds in nascent polypeptides are thought to be formed by ER-resident PDI family proteins. However, how these proteins distinguish between different substrate polypeptides is not well-understood. Among them, ER-60 is a protein for which the means of recognizing substrates has been elucidated. ER-60 has been shown to catalyze the oxidative folding of N-glycosylated proteins by using CNX or CRT as a subunit for substrate binding (*20*−*25*). However, the details of the mechanism of interaction of ER-60 with these molecular chaperones remained unclear. In this study, we demonstrated that the domain structure of ER-60 comprised two catalytic domains, a and a′, and two noncatalytic domains, b and b′. The sites of cleavage on limited proteolysis were mapped to the three boundary regions between the putative a, b, b′, and a′ domains deduced by alignment with the primary structure of PDI. Although the predicted domain boundaries of ER-60 coincided with the results obtained on limited proteolysis, the b and ab domain proteins were expressed as unfolded proteins in *E. coli*. However, a portion of the b domain in the wild-type ER-60 protein or fragment abb′ was shown to be folded. In addition, recombinant fragment b′

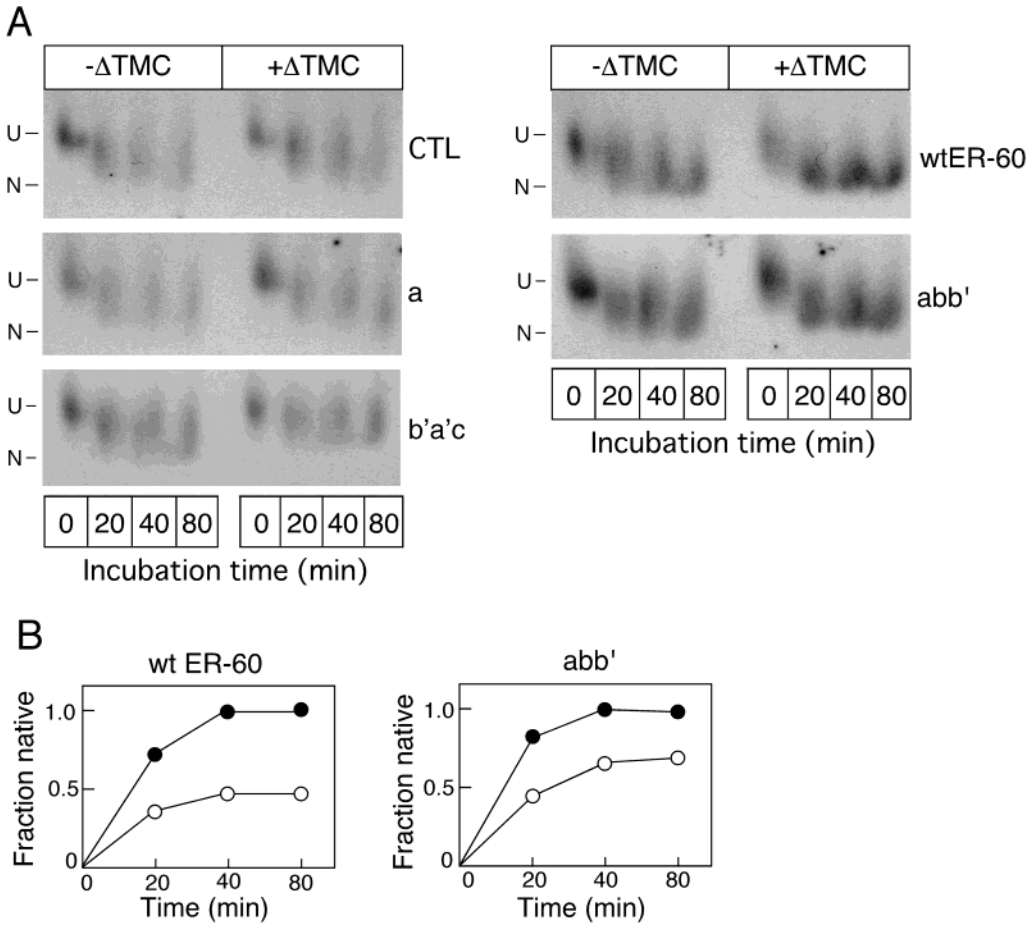

FIGURE 7: Refolding of monoglucosylated RNase B catalyzed by recombinant fragments of ER-60 with or without ΔTMC. (A) Refolding of monoglucosylated RNase B was carried out in the absence (CTL) or presence of wild-type ER-60 (wt ER-60), a, abb′, or b′a′c, with (+ΔTMC) or without (−ΔTMC) ΔTMC, as described under the Experimental Procedures. The reaction was terminated after the indicated times, and then the conformation of the monoglucosylated RNase B was examined by nondenaturing PAGE, followed by fluorography. U and N indicate the unfolded and native forms of RNase B, respectively. (B) Native monoglucosylated RNase B folded in the presence of wt ER-60 or abb′ with (●) or without (○) ΔTMC was quantified by densitometry of the autoradiograms shown in A.

was expressed as a folded protein in *E. coli*. These results suggest that the b region is an independent domain and that the presence of b′ is essential for folding and/or stabilization of the b domain in the folded state under the experimental conditions used. In contrast to the structural lability of fragment b of ER-60, recombinant fragment b of PDI was expressed in *E. coli* as a folded polypeptide (*38*, *39*, *60*). Whereas the a and a′ domains of ER-60 show significant sequence identity to the a and a′ domains of PDI, the homology between the b and b′ domains of ER-60 and PDI is low. Although the b and b′ domains have no enzymatic activity, they may play critical roles in diverse biological functions. The b′ domain of PDI has been indicated to be required for its substrate binding (*40*), its chaperone activity (*40*, *41*), and its association with prolyl 4-hydroxylase as a subunit of this enzyme (*61*). On the other hand, the b and b′ domains of ER-60 are unlikely to be concerned with its substrate binding. In this study, fragments a and a′c of ER-60 expressed in *E. coli* showed activities almost equivalent to half of the oxidative-refolding activity of wild-type ER-60, and extension from a or a′c to abb′ or b′a′c had little effect on their activities. Furthermore, it was shown that the b′ domain of ER-60 was unable to substitute for the b′ domain of PDI in the association with prolyl 4-hydroxylase (*61*). Rather, the b and b′ domains of ER-60 are likely to be important as binding sites for CNX or CRT. Association of wild-type ER-60 and fragment abb′ with ΔTMC or CNX was detected on SPR analysis, whereas no or very slight association of fragments a, a′c, b′, and b′a′c with ΔTMC was observed.

Furthermore, the addition of ΔTMC to the oxidative-refolding assay system enhanced the activities of wild-type ER-60 and fragment abb′ but did not enhance that of fragment a and b′a′c. Hence, both the b and b′ domains are assumed to provide the binding site(s) for CNX and CRT. However, the contribution of the a domain to the association with CNX or CRT remains unclear. Unfortunately, fragment bb′ or bb′a′c was not expressed in *E. coli* for an unknown reason. Hence, whether the b and b′ domains are sufficient for the association with CNX and CRT remains to be elucidated. The association of ER-60 with these molecular chaperones functions not only in the folding of a nascent polypeptide, but also in the dynamic control of ER Ca^{2+} homeostasis. ER-60 molecules recruited by CRT have been indicated to modulate Ca^{2+} oscillation through oxidation of cysteine residues located in intraluminal loop 4 of sarco ER calcium ATPase (*62*).

The affinity of PDI to a substrate has been reported to be regulated by the redox state of its CGHC motifs (*63*). Thus, in the reduced state, PDI binds to the A chain of cholera toxin, and in the oxidized state, PDI releases it. On the other hand, no difference was detected on SPR assaying in the

affinity of ER-60 to ΔTMC, with there being no dependence on the reduced or oxidized form of ER-60. Though ER-60 and PDI are speculated to have evolved from a common ancestor (*34*), the functions of the b and b′ domains of ER-60 are markedly different from those of the b and b′ domains of PDI.

ACKNOWLEDGMENT

We greatly thank Dr. Makoto Kito, Emeritus Professor of Kyoto University, for the valuable advice and warm encouragement.

REFERENCES

1. Freedman, R. B., Hirst, T. R., and Tuite, M. F. (1994) Protein disulfide isomerase: Building bridges in protein folding, *Trends Biochem. Sci. 19*, 331−336.
2. Creighton, T. E., Zapun, A., and Darby, N. J. (1995) Mechanisms and catalysts of disulfide bond formation in proteins, *Trends Biotechnol. 13*, 18−23.
3. Urade, R., Nasu, M., Moriyama, T., Wada, K., and Kito, M. (1992) Protein degradation by the phosphoinositide-specific phospholipase Cα family from rat liver endoplasmic reticulum, *J. Biol. Chem. 267*, 15152−15159.
4. Oliver, J. D., van der Wal, F. J., Bulleid, N. J., and High, S. (1997) Interaction of the thiol-dependent reductase ERp57 with nascent glycoproteins, *Science 275*, 86−88.
5. Lewis, M. J., Mazzarella, R. A., and Green, M. (1986) Structure and assembly of the endoplasmic reticulum: Biosynthesis and intracellular sorting of ERp61, Erp59, and Erp49, three protein components of murine endoplasmic reticulum, *Arch. Biochem. Biophys. 245*, 389−403.
6. Lee, A. S. (1992) Mammalian stress response: Induction of the glucose regulated protein family, *Curr. Opin. Cell Biol. 4*, 267−273.
7. Bourdi, M., Demady, D., Martin, J. L., Jabbour, S. K., Martin, B. M., George, J. W., and Pohl, L. R. (1995) cDNA cloning and baculovirus expression of the human liver endoplasmic reticulum P58: Characterization as a protein disulfide isomerase isoform, but not as a protease or a carnitine acyltransferase, *Arch. Biochem. Biophys. 323*, 397−403.
8. Mobbs, C. V. (1990) HIP-70: An isoform of phosphoinositide-specific phospholipase Cα, *Science 249*, 566−567.
9. Srivastava, S. P., Chen, N., Liu, Y., and Holtzman, J. L. (1991) Purification and characterization of a new isozyme of thiol:protein-disulfide oxidoreductase from rat hepatic microsomes, *J. Biol. Chem. 266*, 20337−20344.
10. Chaudhuri, M. M., Tonin, P. N., Lewis, W. H., and Srinivasan, P. R. (1992) The gene for a novel protein, a member of the protein disulfide isomerase/form I phosphoinositide-specific isomerase C family, is amplified in hydroxyurea-resistant cells, *Biochem. J. 281*, 645−650.
11. Mazzarella, R. A., Srinivasan, M., Haugejorden, S. M., and Green, M. (1990) ERp72, an abundant luminal endoplasmic reticulum protein, contains three copies of the active site sequences of protein disulfide isomerase, *J. Biol. Chem. 265*, 1094−1101.
12. Desilva, M. G., Lu, J., Donadel, G., Modi, W. S., Xie, H., Notkins, A. L., and Lan, M. S. (1996) Characterization and chromosomal localization of a new protein disulfide isomerase, PDIp, highly expressed in human pancreas, *DNA Cell Biol. 15*, 9−16.
13. Hayano, T., and Kikuchi, M. (1995) Molecular cloning of the cDNA encoding a novel protein disulfide isomerase-related protein (PDIR), *FEBS Lett. 372*, 210−214.
14. Anelli, T., Alessio, M., Mezghrani, A., Simmen, T., Talamo, F., Bachi, A., and Sitia, R. (2002) ERp44, a novel endoplasmic reticulum folding assistant of the thioredoxin family, *EMBO J. 21*, 835−844.
15. Alanen, H. I., Williamson, R. A., Howard, M. J., Lappi, A., Jäntti, H. P., Rautio, S. M., Kellokumpu, S., and Ruddock, L. W. (2003) Functional characterization of ERp18, a new endoplasmic reticulum-located thioredoxin superfamily member, *J. Biol. Chem. 278*, 28912−28920.
16. Hirano, N., Shibasaki, F., Sakai, R., Tanaka, T., Nishida, J., Yazaki, Y., Takenawa, T., and Hirai, H. (1995) Molecular cloning of the human glucose-regulated protein ERp57/GRP58, a thiol-dependent reductase: Identification of its secretory form and inducible expression by the oncogenic transformation, *Eur. J. Biochem. 234*, 336−342.
17. Urade, R., and Kito, M. (1992) Inhibition by acidic phospholipids of protein degradation by ER-60 protease, a novel cysteine protease, of endoplasmic reticulum, *FEBS Lett. 312*, 83−86.
18. Urade, R., Oda, T., Ito, H., Moriyama, T., Utsumi, S., and Kito, M. (1997) Functions of characteristic Cys-Gly-His-Cys (CGHC) and Gln-Glu-Asp-Leu (QEDL) motifs of microsomal ER-60 protease, *J. Biochem. 122*, 834−842.
19. Okudo, H., Kito, M., Moriyama, T., Ogawa, T., and Urade, R. (2002) Transglutaminase activity of human ER-60, *Biosci. Biotechnol. Biochem. 66*, 1423−1426.
20. Zapun, A., Darby, N. J., Tessier, D. C., Michalak, M., Bergeron, J. J. M., and Thomas, D. Y. (1998) Enhanced catalysis of ribonuclease B folding by the interaction of calnexin or calreticulin with ERp57, *J. Biol. Chem. 273*, 6009−6012.
21. Oliver, J. D., Roderick, H. L., Llewellyn, D. H., and High, S. (1999) ERp57 functions as a subunit of specific complexes formed with the ER lectins calreticulin and calnexin, *Mol. Biol. Cell 10*, 2573−2582.
22. Elliott, J. G., Oliver, J. D., and High, S. (1997) The thiol-dependent reductase ERp57 interacts specifically with N-glycosylated integral membrane proteins, *J. Biol. Chem. 272*, 13849−13855.
23. Oliver, J. D., van der Wal, F. J., Bulleid, N. J., and High, S. (1997) Interaction of the thiol-dependent reductase ERp57 with nascent glycoproteins, *Science 275*, 86−88.
24. van der Wal, F. J., Oliver, J. D., and High, S. (1998) The transient association of ERp57 with N-glycosylated proteins is regulated by glucose trimming, *Eur. J. Biochem. 256*, 51−59.
25. Molinari, M., and Helenius, A. (1999) Glycoproteins form mixed disulfides with oxidoreductases during folding in living cells, *Nature 402*, 90−93.
26. Wada, I., Rindress, D., Cameron, P. H., Ou, W., Doherty, J. J., II, Louvard, D., Bell, A. W., Dignard, D., Thomas, D. Y., and Bergeron, J. M. (1991) SSRα and associated calnexin are major calcium binding proteins of the endoplasmic reticulum membrane, *J. Biol. Chem. 266*, 19599−19610.
27. Hahn, M., Borisova, S., Schrag, J. D., Tessier, D. C., Zapun, A., Tom, R., Kamen, A. A., Bergeron, J. J. M., Thomas, D. Y., and Cygler, M. (1998) Identification and crystallization of a protease-resistant core of calnexin that retains biological activity, *J. Struct. Biol. 123*, 260−264.
28. Schrag, J. D., Bergeron, J. J. M., Li, Y., Borisova, S., Hahn, M., Thomas, D. Y., and Cygler, M. (2001) The structure of calnexin, an ER chaperone involved in quality control of protein folding, *Mol. Cell 8*, 633−644.
29. Ellgaard, L., Riek, R., Braun, D., Herrmann, T., Helenius, A., and Wüthrich, K. (2001) Three-dimensional structure topology of the calreticulin P-domain based on NMR assignment, *FEBS Lett. 488*, 69−73.
30. Ellgaard, L., Riek, R., Herrmann, T., Güntert, P., Braun, D., Helenius, A., and Wüthrich, K. (2001) NMR structure of the calreticulin P-domain, *Proc. Natl. Acad. Sci. U.S.A. 98*, 3133−3138.
31. Frickel, E., Riek, R., Jelesarov, I., Helenius, A., Wüthrich, K., and Ellgaard, L. (2001) TROSY−NMR reveals interaction between ERp57 and the tip of the calreticulin P-domain, *Proc. Natl. Acad. Sci. U.S.A. 99*, 1954−1959.
32. Leach, M. R., Cohen-Doyle, M. F., Thomas, D. Y., and Williams, D. B. (2002) Localization of the lectin, ERp57 binding, and polypeptide binding sites of calnexin and calreticulin, *J. Biol. Chem. 277*, 29686−29697.
33. Ferrari, D. M., and Söling, H. (1999) The protein disulfide-isomerase family: Unravelling a string of folds, *Biochem. J. 339*, 1−10.
34. Kanai, S., Toh, H., Hayano, T., and Kikuchi, M. (1998) Molecular evolution of the domain structures of protein disulfide isomerases, *J. Mol. Evol. 47*, 200−210.
35. Freedman, R. B., Klappa, P., and Ruddock, L. W. (2002) Protein disulfide isomerases exploit synergy between catalytic and specific binding domains, *EMBO Rep. 3*, 136−140.
36. Kemmink, J., Darby, N. J., Dijkstra, K., Nilges, M., and Creighton, T. E. (1996) Structure determination of the N-terminal thioredoxin-like domain of protein disulfide isomerase using multidimensional heteronuclear $^{13}C/^{15}N$ NMR spectroscopy, *Biochemistry 35*, 7684−7691.
37. Silvennoinen, L., Karvonen, P., Koivunen, P., Myllyharju, J., Kivirikko, K., and Kilpeläinen, I. (2001) Letter to the editor:

Assignment of ^{1}H, ^{13}C, and ^{15}N resonances of the a′ domain of ERp57, *J. Biomol. NMR 20*, 385−386.
38. Kemmink, J., Darby, N. J., Dijkstra, K., Nilges, M., and Creighton, T. E. (1997) The folding catalyst protein disulfide isomerase is constructed of active and inactive thioredoxin modules, *Curr. Biol. 7*, 239−245.
39. Kemmink, J., Klaas, D., Mariani, M., Scheek, R. M., Penka, E., Nilges, M., and Darby, N. J. (1999) The structure in solution of the b domain of protein disulfide isomerase, *J. Biomol. NMR 13*, 357−368.
40. Klappa, P., Ruddock, L. W., Darby, N. J., and Freedman, R. B. (1998) The b′ domain provides the principal peptide-binding site of protein disulfide isomerase but all domains contribute to binding of misfolded proteins, *EMBO J. 17*, 927−935.
41. Klappa, P., Koivunen, P., Pirneskoski, A., Karvonen, P., Ruddock, L. W., Kivirikko, K. I., and Freedman, R. B. (2000) Mutations that destabilize the a′ domain of human protein-disulfide isomerase indirectly affect peptide binding, *J. Biol. Chem. 275*, 13213−13218.
42. Chong, S., Montello, G. E., Zhang, A., Cantor, E. J., Liao, W., Xu, M., and Benner, J. (1998) Utilizing the C-terminal cleavage activity of a protein splicing element to purify recombinant proteins in a single chromatographic step, *Nucleic Acids Res. 26*, 5109−5115.
43. Suzuki, Y., Yoshitomo-Nakagawa, K., Maruyama, K., Suyama, A., and Sugano, S. (1997) Construction and characterization of a full length-enriched and a 5′-end-enriched cDNA library, *Gene 200*, 149−156.
44. Ou, W., Bergeron, J. J. M., Li, Y., Kang, C. Y., and Thomas, D. Y. (1995) Conformational changes induced in the endoplasmic reticulum luminal domain of calnexin by Mg-ATP and Ca^{2+}, *J. Biol. Chem. 270*, 18051−18059.
45. Ou, W., Cameron, P. H., Thomas, D. Y., and Bergeron, J. J. M. (1993) Association of folding intermediates of glycoproteins with calnexin during protein maturation, *Nature 364*, 771−776.
46. Creighton, T. E. (1979) Intermediates in the refolding of reduced ribonuclease A, *J. Mol. Biol. 129*, 411−431.
47. Okudo, H., Urade, R., Moriyama, T., and Kito, M. (2000) Catalytic cysteine residues of ER-60 protease, *FEBS Lett. 465*, 145−147.
48. Creighton, T. E. (1977) Kinetics of refolding of reduced ribonuclease, *J. Mol. Biol. 113*, 329−341.
49. Lyles, M. M., and Gilbert, H. F. (1991) Catalysis of the oxidative folding of ribonuclease A by protein disulfide isomerase: Dependence of the rate on the composition of the redox buffer, *Biochemistry 30*, 613−619.
50. Zapun, A., Petrescu, S. M., Rudd, P. M., Dwek, R. A., Thomas, D. Y., and Bergeron, J. J. M. (1997) Conformation-independent binding of monoglucosylated ribonuclease B to calnexin, *Cell 88*, 29−38.
51. Trombetta, S. E., and Parodi, A. J. (1992) Purification to apparent homogeneity and partial characterization of rat liver UDP-glucose: glycoprotein glucosyltransferase, *J. Biol. Chem. 267*, 9236−9240.
52. Reisfeld, R. A., Lewis, U. J., and Williams, D. E. (1962) Disk electrophoresis of basic proteins and peptides on polyacrylamide gels, *Nature 195*, 281−283.
53. Chou, P. Y., and Fasman, G. D. (1978) Prediction of the secondary structure of proteins from their amino acid sequence, *Adv. Enzymol. Relat. Areas Mol. Biol. 47*, 45−148.
54. Xiao, R., Solovyov, A., Gilbert, H. F., Holmgren, A., and Lundström-Ljung, J. (2001) Combinations of protein-disulfide isomerase domains show that there is little correlation between isomerase activity and wild-type growth, *J. Biol. Chem. 276*, 27975−27980.
55. Walker, K. W., Lyles, M. M., and Gilbert, H. F. (1996) Catalysis of oxidative protein folding by mutants of protein disulfide isomerase with a single active-site cysteine, *Biochemistry 35*, 1972−1980.
56. Corbett, E. F., Oikawa, K., Francois, P., Tessier, D. C., Kay, C., Bergeron, J. J. M., Thomas, D. Y., Krause, K., and Michalak, M. (1999) Ca^{2+} regulation of interaction between endoplasmic reticulum chaperones, *J. Biol. Chem. 274*, 6203−6211.
57. Corbett, E. F., Michalak, K. M., Oikawa, K., Johnson, S., Campbell, I. D., Eggelton, P., Kay, C., and Michalak, M. (2000) The conformation of calreticulin is influenced by the endoplasmic reticulum luminal environment, *J. Biol. Chem. 275*, 27177−27185.
58. Reddy, A. G., Devi, B. G., Rao, S. B., and Gupta, P. D. (1989) Localization of intracellular zinc under conditions of altered permeability control of the plasma membrane, *Cytobios 60*, 21−26.
59. Ihara, Y., Cohen-Doyle, M. F., Saito, Y., and Williams, D. B. (1999) Calnexin discriminates between protein conformational states and functions as a molecular chaperone in vitro, *Mol. Cell 4*, 331−341.
60. Darby, N. J., Kemmink, J., and Creighton, T. E. (1996) Identifying and characterizing a structural domain of protein disulfide isomerase, *Biochemistry 35*, 10517−10528.
61. Pirneskoski, A., Ruddock, L. W., Klappa, P., Freedman, R. B., Kivirikko, K. I., and Koivunen, P. (2001) Domains b′ and a′ of protein disulfide isomerase fulfill the minimal requirement for function as a subunit of proryl 4-hydoxylase, *J. Biol. Chem. 276*, 11287−11293.
62. Li, Y., and Camacho, P. (2004) Ca^{2+}-dependent redox modulation of SERCA 2b by ERp57, *J. Cell Biol. 164*, 35−46.
63. Tsai, B., Rodighiero, C., Lencer, W. I., and Rapoport, T. A. (2001) Protein disulfide isomerase acts as a redox-dependent chaperone to unfold cholera toxin, *Cell 104*, 937−948.

BI0493315